Atmospheric Research 259 (2021) 105658

Contents lists available at ScienceDirect

Atmospheric Research

journal homepage: www.elsevier.com/locate/atmosres

Summer afternoon precipitation associated with wind convergence near the Himalayan glacier fronts

Changgui Lin [a,b,*], Kun Yang [c,d], Deliang Chen [a,*], Nicolas Guyennon [e], Raffaella Balestrini [f], Xiaoxin Yang [d,g], Sunil Acharya [h], Tinghai Ou [a], Tandong Yao [d,g], Gianni Tartari [f], Franco Salerno [f]

[a] Regional Climate Group, Department of Earth Sciences, University of Gothenburg, Gothenburg, Sweden
[b] Rossby Centre, Swedish Meteorological and Hydrological Institute, Norrköping, Sweden
[c] Ministry of Education Key Laboratory for Earth System Modelling and Department of Earth System Science, Tsinghua University, Beijing, China
[d] CAS Center for Excellence in Tibetan Plateau Earth System Sciences, Chinese Academy of Sciences, Beijing, China
[e] Water Research Institute, National Research Council (IRSA-CNR), Rome, Italy
[f] Water Research Institute, National Research Council (IRSA-CNR), Brugherio, Italy
[g] Key Laboratory of Tibetan Environmental Changes and Land Surface Process, Institute of Tibetan Plateau Research, Chinese Academy of Sciences, Beijing, China
[h] Central Department of Hydrology and Meteorology, Tribhuvan University, Kathmandu, Nepal

ARTICLE INFO

Keywords:
Glacier-air interactions
Himalayan glaciers
Glacier mass balance
Feedback mechanism
Elevational dependence

ABSTRACT

Little is known about the effects of glacier-air interactions on the Himalayan glacier mass balance. Until this knowledge gap is filled, a reliable projection of the future changes in the Himalayan glaciers is hardly possible. Here, we describe the drying effect of the katabatic winds on the up-valley summer monsoon flows by creating favorable conditions for local convergence-induced precipitation to occur near the glacier fronts. We postulate that this retarding effect on the up-valley monsoon flows results in a negative feedback mechanism mediated by glacier-air interactions, in which glacial retreat pushes precipitation upwards as the down-valley katabatic winds weaken, resulting in greater local precipitation and enhanced snow accumulation across the upper parts of the Himalayan glaciers. Our analyses are based on the exclusive data recorded in the Khumbu valley and the Langtang valley in the Nepalese Himalayas. These data revealed higher afternoon precipitation in summer associated with surface wind convergence near the glacier fronts and a sharp decrease in the temperature lapse rate over the glacier surfaces. The principle of the observed phenomena was proven by our high-resolution modeling sensitive experiment, which involved two simulations, one with the present glaciers and the other without. This numerical experiment also supports the proposed negative feedback. Furthermore, we report a low deuterium excess near the glacier fronts, indicating below-cloud re-evaporation facilitated by the local convergence induced by the dry katabatic winds. Our study suggests that current models may overestimate the retreat of Himalayan glaciers because they have completely ignored the glacier-air interactions.

1. Introduction

As major elements of Asia's so-called water tower, the Himalayan glaciers contribute significantly to and regulate the water supply in the downstream regions inhabited by a large portion of the world's population (Immerzeel et al., 2010; Kaser et al., 2010; Lutz et al., 2014; Immerzeel et al., 2020). Mass loss from these glaciers poses substantial socio-economic and ecological threats through associated reductions in water availability (Barnett et al., 2005) and increasing contributions to eustatic sea-level rise (Radić and Hock, 2011; Gardner et al., 2013). The rapid retreat of the Himalayan glaciers in recent decades has been primarily driven by climatic warming (Bolch et al., 2012; Yao et al., 2012; Maurer et al., 2019). Therefore, their future fate is of great concern; and this scientific challenge has become the focus of heated debate (Bolch et al., 2012).

Efforts have been made to project future glacier mass changes both globally and with a specific regional focus on the Himalayas (e.g., Kraaijenbrink et al., 2017; Hock et al., 2019; Shannon et al., 2019). Such

* Corresponding authors at: Regional Climate Group, Department of Earth Sciences, University of Gothenburg, Gothenburg, Sweden.
E-mail addresses: mapulynn@gmail.com (C. Lin), deliang@gvc.gu.se (D. Chen).

https://doi.org/10.1016/j.atmosres.2021.105658
Received 6 March 2021; Received in revised form 27 April 2021; Accepted 27 April 2021
Available online 1 May 2021

projections yield valuable insights into the likely fates of glaciers under a range of scenarios. The usual two approaches adopt either physics-based or statistical glacier models that are forced using existing climate projections. A greater concern regarding the aforementioned approaches is that glacier-air interactions are not taken into account. In the current models used for projections, glaciers are considered to respond solely to local climate changes, whereas in reality, the changes in glacier extent alter the surface energy balance and thus the local climate, which in turn feeds back into the glacier mass balance. Therefore, possible feedback mechanisms within the glacier-climate system may amplify or dampen glacial retreat or advance. These feedback mechanisms must be understood before reliable projections can be made.

Here, we explore the role played by glacier-air interactions in modulating the mass balance of the Himalayan glaciers to shed light on their fate under future climatic warming. Specifically, for the first time, a negative feedback mechanism mediated by glacier-air interactions is postulated based on our empirical knowledge. Our hypothesis is assessed from multiple perspectives: i) analyses based on in situ meteorological measurements; ii) sensitivity studies based on high-resolution modeling; and iii) information derived from the stable isotope composition of precipitation. In order of priority, we aim to demonstrate the proposed negative feedback mechanism, and to provide a first-order estimate of its strength under the current climate conditions. The implications of this feedback for glacier modeling are also discussed, in particular the fact that the existing projections ignore glacier-air interactions.

2. Hypothesis: a negative feedback mechanism

In summer, the daytime up-valley winds over the southern slopes of the Himalayas push the warm, moist monsoonal air mass northwards towards higher elevations, which is significant for the precipitation both in the Himalayas and on the Tibetan Plateau (Lin et al., 2018). Meanwhile, cooling of the air over glacial surfaces generates katabatic winds (i.e., cold, dense air flowing downhill under the force of gravity; also called glacier winds), which counteract the daytime up-valley winds near glacier fronts. We suppose that this front-like convergence can force the warm, moist monsoonal air mass to uplift, which favors precipitation around the convergence zone (near the glacier fronts); on the other hand, it may prevent the monsoonal flows from advancing to higher elevations, reducing the moisture supply for precipitation over the upper part of the glaciers and resulting in a negative anomaly in the local glacier mass budget. Fig. 1 presents a graphic illustration of this mechanism.

The central and eastern Himalayan glaciers are of the summer-accumulation type (Ageta and Higuchi, 1984) and are strongly influenced by the Asian summer monsoon, which brings more than 80% of the total precipitation in the region (Bookhagen and Burbank, 2010). Therefore, the mechanism proposed above could be vital in modulating precipitation patterns and consequently the Himalayan glacier mass balance.

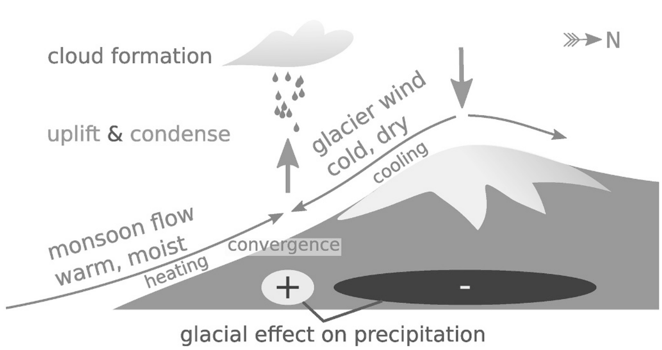

Fig. 1. Hypothesized effect of glacier-air interactions on local precipitation. Arrows show the motion of air masses; plus and minus signs indicate the promotion or suppression of precipitation, respectively.

3. Data and methods

3.1. Meteorological observation network and data processing

Meteorological measurements at the elevations of glaciers provide essential information on local-scale glacier-air interactions. The PYRAMID Observatory Laboratory (Fig. 2a) provides such data (Salerno et al., 2015), but it is impaired by the incomplete nature of records caused by the harsh and remote environment. This observation network consists of six automatic weather stations distributed at elevations of 2660–7986 m above sea level (asl) along the Khumbu valley in the Mt. Everest region (Nepal). Lukla (2660 m asl) and Namche (3570 m asl) are located in a landscape dominated by forests; Pheriche (4260 m asl) is located above the treeline, in alpine tundra; Pyramid (5035 m asl) is near glacial fronts; Kala Patthar (5600 m asl) represents the mean elevation of glaciers in the region; and the South Col of Mt. Everest (7986 m asl) is close to the summit of Mt. Everest (this station was excluded from our analysis since no precipitation data were recorded). An overview of the stations is provided in Table 1 presents.

This unique dataset contains precipitation, near-surface wind, and air temperature data. Precipitation was measured with conventional heated tipping buckets. We revisited the elevational dependence and diurnal cycles of these meteorological parameters following the method of Yang et al. (2018) but with a focus on the summer season (June–August; the mature season of the South Asian monsoon). The summer mean diurnal cycles were derived from the hourly records (available from 2007 to 2011) under the assumption that data are missing at random. Then, the summer mean values were obtained from the diurnal cycle data. We used the meridional wind data to approximate the along-valley wind in the analysis since the Khumbu valley is oriented approximately south to north. The surface air temperature lapse rate (TLR) was calculated as the difference in surface air temperature between lower and higher stations, divided by their elevation difference. A positive TLR indicates that surface air temperature decreases with increasing elevation. In particular, the differences in the diurnal evolution of TLR above and below the glacier fronts may reveal the interaction between glacier winds and monsoonal flows, and therefore are of interest in this study. Yang et al. (2018) described the details of the quality checks and data processing, as well as the sensor information; particularly, precipitation was measured with OttPluvio 400 (unshielded) buckets.

In order to determine if the phenomena observed in the Khumbu valley are common in the central Himalayas, we also conducted similar analyses focused on the summer season based on the meteorological data recorded during 2012–2014 at two stations in the Langtang valley (Fig. 2b and the second part of Table 1). The orography there is oriented approximately west to east. Along the valley, the two stations are Kyanging (3862 m asl) and Yala Base Camp (5090 m asl). The latter is located just below Yala Glacier. Shea et al. (2015) provides the details of the quality checks and data processing, as well as the sensor information (in fact the same as PYRAMID Observatory Library).

3.2. Design of the modeling experiments

A high-resolution model is required to adequately represent and resolve the relevant processes at small spatial scales. The Weather Research Forecasting (WRF) model (Skamarock et al., 2008) features state-of-the-art numeric and comprehensive physical parameterizations, and is suitable for simulation across a variety of horizontal and vertical scales. The WRF has been successfully applied in previous studies focusing on the Himalayas (e.g., Collier et al., 2015; Norris et al., 2017; Karki et al., 2017; Lin et al., 2018; Potter et al., 2018; Ren et al., 2020). For example, by comparing WRF simulations with three horizontal

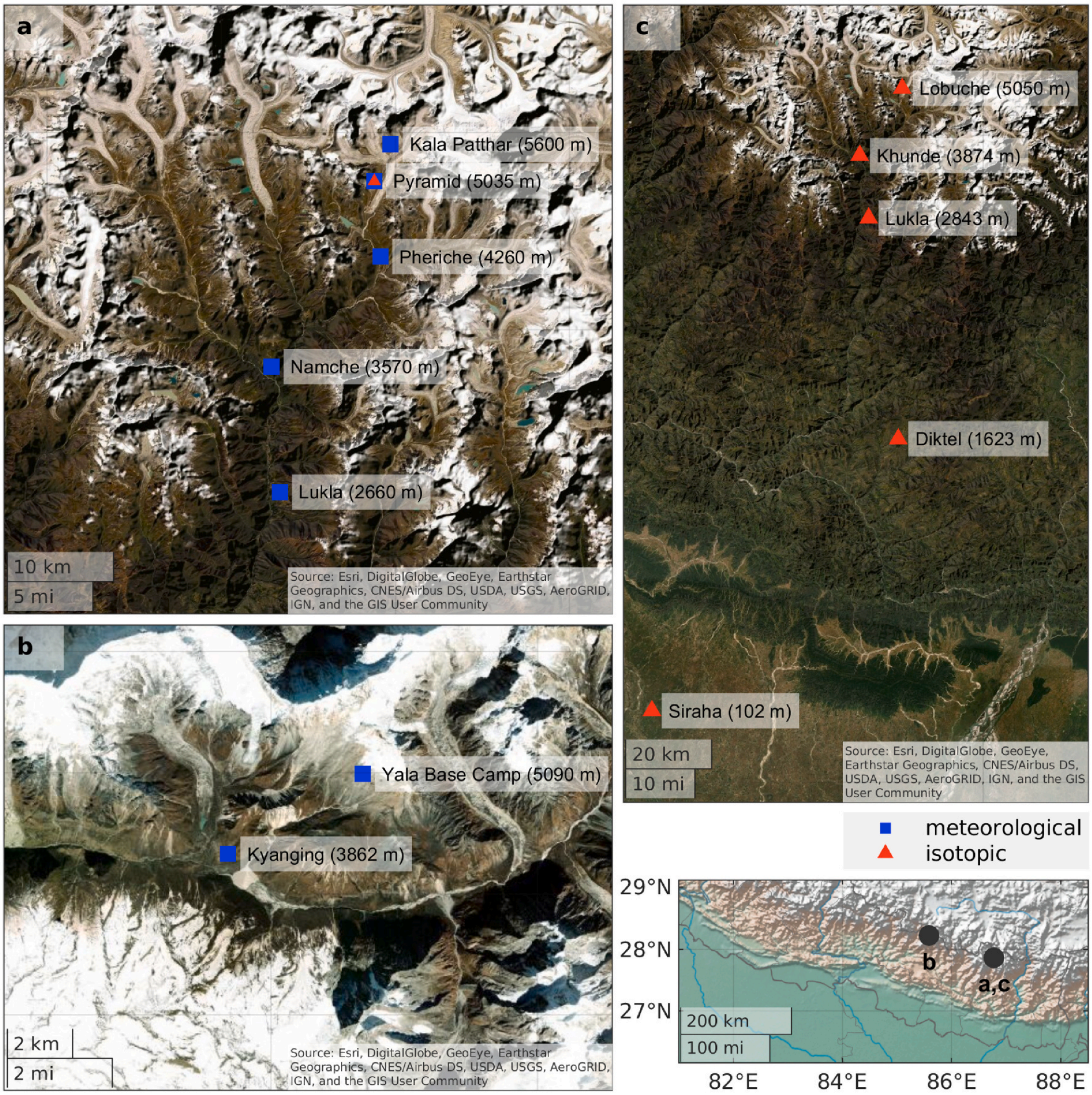

Fig. 2. Focused maps showing the spatial distribution of stations used in this study: (**a**) of the PYRAMID Observatory Laboratory in the Khumbu valley; (**b**) of the meteorological observation network in the Langtang valley; and (**c**) of the precipitation sampling network for stable isotopes in the Kunmbu valley. Blue squares stand for stations with meteorological observations while red triangles denote stations with precipitation sampling for stable isotopes. A zoomed-out map is presented in the bottom-right corner.

resolutions (30, 10, and 2 km), Lin et al. (2018) concluded that the ability of the 2-km simulation to resolve glacier winds is a likely reason for the improvements in simulating water vapor transport across the central Himalayas. Indeed, modeling climatic processes over mountainous glaciers poses substantial challenges, especially in the Himalayas due to the extreme topographical relief. Rather than modeling phenomena over a single glacier or across all of the Himalayan glaciers, a proper approach is to focus on one or two groups of large glaciers in the central Himalayas, as was done by the 2-km simulation conducted by Lin et al. (2018). Therefore, we utilized the 2-km simulation which adopts the current glacier conditions as the control (i.e., 'glacier case'). Three one-way nested domains (Supplementary Fig. S1) were set to smoothly refine the ERA-interim reanalysis (Dee et al., 2011), which has a spatial resolution of 0.75°, to the 2-km grid spacing. The simulation began at 00:00 UTC on 26 May 2015 and ended at 00:00 UTC on 1 September 2015. The simulation of the summer season was analyzed (i.e., with the first 6 days regarded as the model's spin-up time). Fig. 3 presents the region of investigation for the WRF modeling experiment. The details of the model configuration are presented in Supplementary Table S1.

In the sensitivity simulation (i.e., 'non-glacier case'), in order to assess the effects of the complete loss of glaciers, the following approach was applied: i) the grid cells classified as glacierized area (with land use type specified as 'SNOW/ICE'; Fig. 3) were reclassified as bare ground; ii) the existing snow in the initial field was removed; and, iii) the solid precipitation in the model was forced to be liquid, so as to fully represent a surface free of cooling effect. By this approach, it implies that both grid cells with land use type specified as 'SNOW/ICE' and snow cover at high elevations were treated as glaciers in respect of the fact that they both cause surface cooling. Apart from this, both the control and sensitivity runs shared the same lateral boundary conditions provided by the simulation of the medium-resolution domain (D02 in Supplementary Fig. S1). The differences between the control and sensitivity simulations indicate the effects of glacier-air interactions (with contrasting values indicating the effects of a complete loss of glaciers). Rather than following the experimental design of a previous study (Mölg et al., 2012) which examined the contribution of the land cover changes to glacier loss on Kilimanjaro, we focused on testing our hypothesis. Thus, we did not apply nudging in the modeling experiments of Mölg et al. (2012) but

Table 1
Overview of the meteorological and isotopic observation networks (with location and observation period in parentheses).

Station	Latitude (°N)	Longitude (°E)	Elevation (m asl)	Landscape feature
PYRAMID Observatory Laboratory (Khumbu; 2007–2011)				
Kala Patthar	27.99	86.83	5600	Glaciers
Pyramid[a]	27.96	86.81	5035	Glacier fronts
Pheriche	27.90	86.82	4260	Treeline
Namche	27.80	86.72	3570	Forests
Lukla	27.70	86.72	2660	Forests
Meteorological observation network (Langtang; 2012–2014)				
Yala Base Camp	28.23	85.61	5090	Glacier fronts
Kyanging	28.21	85.57	3862	Grass
Precipitation sampling network for stable isotopes (Khumbu; 2014–2017)				
Lobuche	27.95	86.81	5050	Glacier fronts
Khunde	27.81	86.71	3874	Treeline
Lukla	27.68	86.73	2843	Forests
Diktel	27.22	86.80	1623	Forests
Siraha	26.65	86.22	102	Forests

[a] with precipitation sampling for stable isotopes.

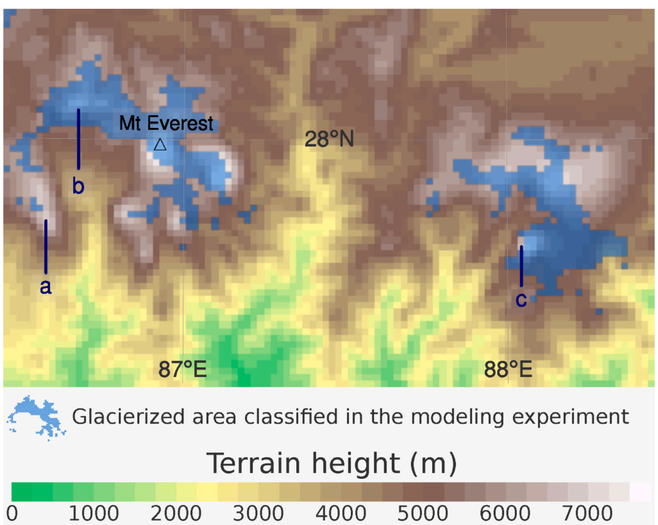

Fig. 3. The region of investigation for the WRF modeling experiment. It should be noted that the grid cells with snow in the initial field may also be outside the classified glacierized area (with land use type SNOW/ICE). Three south-north orientated lines labeled 'a', 'b', and 'c' were set for analyzing the elevational dependence and diurnal cycle of simulated temperature lapse rate hereafter.

gave the model as much freedom as possible, because nudging may violate the conservation of energy and mass.

3.3. Precipitation sampling for stable isotope analysis

The stable water isotopic compositions (e.g., δ^{18}O, δD) refer to the isotopic ratios (heavier to lighter) of the sample relative to those of the standard (Vienna Standard Mean Ocean Water). Deuterium excess (*d*-excess) is a second-order isotopic parameter defined as $\delta D - 8 \cdot \delta^{18}O$ (Dansgaard, 1964), which represents the fractionation between oxygen and hydrogen isotopes during the global water circulation (from the evaporation of ocean water to the gradual rainout from moist air masses). Thus, *d*-excess is considered to be a useful tracer of hydrological processes at regional and global scales (Aemisegger et al., 2014; Masson-Delmotte et al., 2005). Regarding the Himalayan region, for example, a number of studies (e.g., Hren et al., 2009; Ren et al., 2017; Tian et al., 2001, 2005; Yu et al., 2016) have used *d*-excess mostly to determine the moisture sources (or associated atmospheric circulations) according to the seasonality and/or spatial patterns. We investigated whether the *d*-excess in precipitation collected in the Himalayan catchments could be used to trace the processes associated with the hypothesized mechanism illustrated in Fig. 1.

Two sources of stable isotopes were used in our isotopic analyses, and both were located in the Khumbu valley.

One is the precipitation sampling network for stable isotopes in the Khumbu valley (Fig. 2c and the third part of Table 1), managed by the Key Laboratory of Tibetan Environmental Changes and Land Surface Processes, Chinese Academy of Sciences. It consists of five stations: Siraha (102 m asl), Diktel (1623 m asl), Lukla (2843 m asl), Khunde (3874 m asl), and Lobuche (5050 m asl). The precipitation samples were collected immediately after each complete precipitation event using a deep bucket of 15 cm in diameter placed in an open field. Only precipitation events with amounts exceeding 0.1 mm were considered. Then, samples were stored until the analysis for isotopes, which was conducted using Picarro-L2130i Wavelength-Scanned Cavity Ring-Down Spectroscopy (WS-CRDS). The precision is ±0.15‰ and ±0.50‰ for δ^{18}O and δD, respectively. Since the precipitation samples were event-based, the duration of each sample varied. In the data processing, simple mean values were calculated for days with more than one precipitation event. Otherwise, a precipitation event lasting over one day was considered to be a single precipitation event. For further details, refer to Acharya (2018). During the summer monsoon season (June–September) from 2014 to 2017, the sample size was 122, 205, 84, 53, and 62 for Siraha, Diktel, Lukla, Khunde, and Lobuche, respectively. The elevational dependence of *d*-excess during the summer monsoon season was analyzed based on the isotopes at the five sites.

The other source of stable isotopes is Pyramid station of the PYRAMID Observatory Laboratory. The isotopic data are available from 12th July 2012 to 22nd August 2014. Rain water was sampled daily at 9:00 AM (time specified herein referring to Nepal Local Time for observation and UTC + 6 for simulation) using a wet-only sampler (MTX, Bologna, Italy) equipped with a polyethylene vessel of 30 cm in diameter. Thus, each data point therefore represents the cumulative precipitation of the previous 24 h. δ^{18}O, δD were determined by WS-CRDS at the Institute of Arctic and Alpine Research, University of Colorado at Boulder, USA. The uncertainties associated with δ^{18}O, δD are ±0.20‰ and ±1.00‰, respectively. For further details, refer to Balestrini et al. (2016). A total of 63 samples were collected in the summer monsoon season. Based on the isotopic data and hourly precipitation data at Pyramid and Pheriche, the association between *d*-excess and the 'glacial effect' on precipitation (i.e., due to the interaction between glacier winds and monsoonal flows) was examined. According to our hypothesis as described in Section 2 and illustrated in Fig. 1, *daytime* precipitation around the *glacier fronts* (represented here by the Pyramid station) is favored by the front-like convergence between glacier winds and monsoonal flows. Since the samples were integrated over the previous 24 h, we established the following two criteria for detecting daily precipitation events mainly attributed to the glacial effect: i) more precipitation was detected near the glacier (Pyramid) than at a lower elevation (Pheriche) during the daytime period (11:00–20:00, previous day), and ii) events near the glacier (Pyramid) had higher *daytime* precipitation than *nighttime* (21:00–10:00, current day) precipitation. Specifically, the measures for these two criteria (C_i and C_{ii}; associated with the elevational dependence and the diurnal cycle, respectively) are expressed as follows:

$$C_i = \frac{P_{Pyramid}^{daytime}}{P_{Pyramid}^{daytime} + P_{Pheriche}^{daytime}}; \quad (1)$$

$$C_{ii} = \frac{P_{Pyramid}^{daytime}}{P_{Pyramid}^{daytime} + P_{Pyramid}^{nighttime}}, \quad (2)$$

where P is amount of precipitation.

To determine if the mean of *d*-excess in precipitation in one group is significantly less than that in another group, the one tailed two-sample Student's *t*-test was applied. Specifically, we are interested in the *d*-excess difference between stations located close to and far away from glacier fronts, and that between glacier-effect ($C_i \geq 50\%$ and $C_{ii} \geq 50\%$) and non-glacier-effect ($C_i < 50\%$ and $C_{ii} < 50\%$) precipitation events. It is appropriate to assume that *d*-excess values of different groups are from populations with equal variances. To further verify that the *d*-excess difference is probably related to the partial evaporation below cloud base, we also tested the difference in relative humidity (near surface) and cloud base altitude between glacier-effect and non-glacier-effect precipitation events. The cloud base altitude was estimated in terms of the temperature difference between the surface and the lifting condensation level ($T_L - T_S$), which is more closely connected to the partial evaporation below cloud base. The following equation (Bolton, 1980) was used to calculate temperature at the lifting condensation level (T_L in K):

$$T_L = \frac{1}{\frac{1}{T_S - 55} - \frac{ln(RH/100)}{2840}} + 55, \tag{3}$$

where T_S is near-surface temperature (K) and RH is near-surface relative humidity (%).

4. Results

4.1. Evidence from meteorological observations

The horizontal bars in Fig. 4 show the summer mean daily precipitation recorded at the five stations distributed along the Khumbu valley. The greatest precipitation was recorded at the lowest station, but a notable peak was observed at Pyramid (5050 m asl) which deviates from the relatively uniform profile of precipitation. Furthermore, when compared to stations located at lower elevations, Pyramid clearly stands out as having a higher portion of daytime (11:00–20:00) precipitation associated with an afternoon peak of precipitation recorded only at this station among the three presented in Fig. 5b. It is worth mentioning that the diurnal cycle of summer precipitation recorded at Kala Patthar could fail to represent reality due to the measurement issue that late-morning data may record the nighttime snowfall and is therefore not presented.

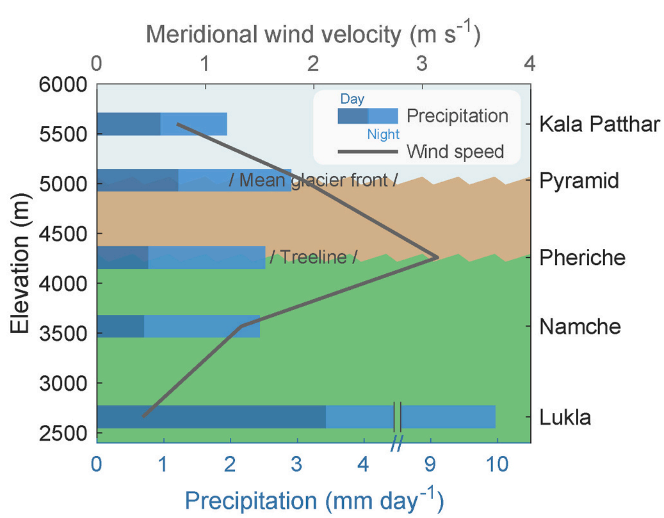

Fig. 4. Elevational dependence of precipitation and meridional wind velocity in summer (June–August) during 2007–2010. Daytime (11:00–20:00) and nighttime (21:00–10:00) portions in precipitation are indicated by dark and light blue, respectively. Background colors indicate the elevations associated with the mean landscape features: green as forests, brown as bare ground or alpine tundra, and silver as glaciers.

This higher portion of daytime precipitation at Pyramid is proposed to be a manifestation of the retarding effect of glacial cooling on the daytime up-valley winds, as illustrated in Fig. 1.

The retarding effect is further supported by the observation that the up-valley winds decrease as elevation increases (Fig. 4), which indicates an abnormal convergence of surface air at the elevations enclosing Pyramid, where the landscape is formed by glacier front (Salerno et al., 2017). Fig. 5a shows more details of wind recorded at the five stations. At Kala Patthar, the wind moves downward in the afternoon (from west to east according to the local orography) further manifesting the convergence near Pyramid. In addition, the interaction between glacier winds and warm up-valley flows close to the glacier fronts may disrupt local temperature regimes (Conway et al., 2021; Shaw et al., 2021). Indeed, high variability in the TLR diurnal cycle was observed over the glacier surfaces between Pyramid and Kala Pattar, in contrast to that over the off-glacier surfaces between Lukla and Pyramid (Fig. 5c). This is again considered to be linked to the glacial effect: the cooling effect of glacier contrasting with the surface heating at lower elevations leads to a dramatic increase in TLR after sunrise, promoting the development of cold glacier winds which converge with the warm daytime up-valley monsoonal flows resulting in a notable sharp decrease in TLR from 10:00 to 16:00 local time. As a consequence, the front-like convergence forces the warm, moist monsoonal air mass to uplift, favoring the local precipitation around the convergence zone. By contrast, this uplift may prevent the monsoonal flows from reaching higher elevations, thereby reducing the moisture supply for precipitation over the upper part of glaciers.

The aforementioned phenomena were more visible with the same analyses carried out for the days with precipitation events classified as due to glacier-effect following the two criteria ($C_i \geq 50\%$ and $C_{ii} \geq 50\%$) defined in Sect. 3.3. It is reflected in these facts revealed by Fig. S2: i) a weaker northward wind at Pyramid indicating more likely a convergence here; ii) an afternoon precipitation peak at Pyramid more distinct from the lower stations; and, iii) an even sharper decrease in TLR over the glacier surfaces from 10:00 to 16:00 local time.

Similar phenomena were observed in the Langtang valley. The dominant daytime up-valley winds blow from west to east shaped by the general orography, and they significantly decrease from Kyanging to Yala Base Camp (Fig. 6a) indicating a convergence of air masses enclosing the glacier fronts. Accordingly, greater precipitation was recorded at Yala Base Camp, especially in the afternoon (Fig. 6b). Unfortunately, since no on-glacier station available, we could not investigate the TLR over the glacier surfaces. Likewise to the Khumbu valley, a comparatively low variability in the TLR diurnal cycle is seen over the off-glacier surfaces between Kyanging and Yala Base Camp (Fig. 6b). In particular, we did not observe a sharp decrease in TLR during the afternoon.

4.2. Evidence from high-resolution modeling

According to Fig. 7, the presence of glaciers in the Himalayan range leads to much less precipitation at the glacier-dominated high elevations and an excess, though of small magnitude, sparsely distributed at elevations of 4–5 km that coincide with the glacier fronts. Significant differences in precipitation occur in the local afternoon, indicating a linkage with surface thermal conditions. The model simulations show extreme negative sensible heat fluxes over the snow/ice surfaces, accompanied by strong katabatic winds (the downward anomalies in Fig. 8), especially at local noon. The wind anomalies converge most strongly below the glacier fronts, favoring convection at these locations. The convergence can be further supported by the simulated sharp daytime decrease in TLR over the glacier-dominated high elevations (Fig. 9), which is consistent with the observations in the Khumbu valley (Fig. 5c). This phenomenon is observed from the 'glacier case' and is more patent from the difference between 'glacier case' and 'non-glacier case', indicating that it is caused by the presence of glaciers.

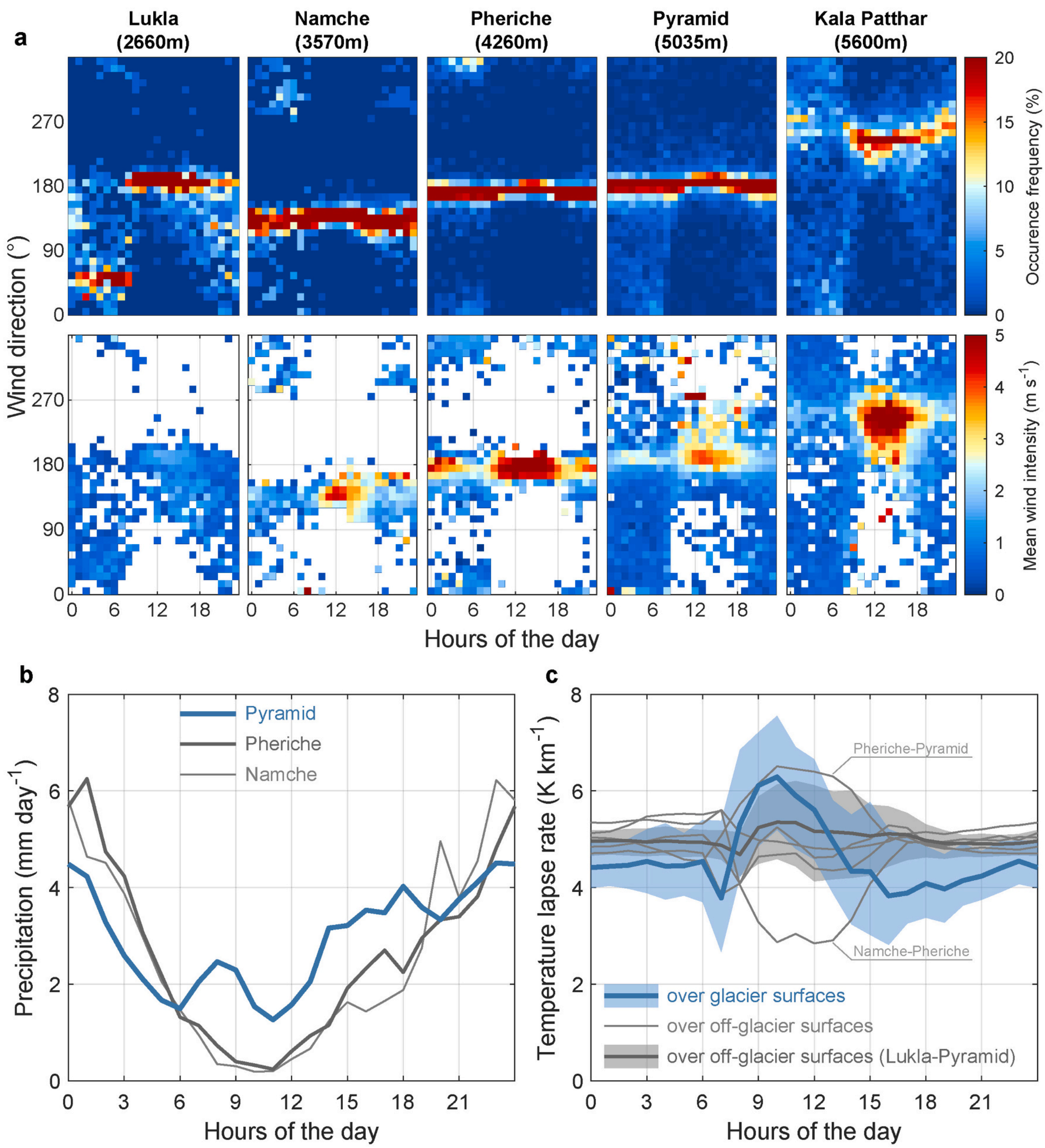

Fig. 5. Diurnal cycle of the three parameters measured in the Khumbu valley in summer (June–August) during 2007–2010: (**a**) occurrence frequency and mean intensity of near-surface wind; (**b**) precipitation; and (**c**) lapse rate of surface air temperature between any combination of two stations. Areas between 25th- and 75th- percentiles are particularly presented for the temperature lapse rate over the glacier surfaces between Pyramid and Kala Pattar and that over the off-glacier surfaces between Lukla and Pyramid.

The retarding effect of glacier winds on the daytime up-valley monsoonal flows is represented in our simulations as the southward anomaly of lateral water vapor flux over the southern Himalayan slopes (Fig. 10; approximately to the south of 28°N). This effect reduces the amount of water vapor reaching the upper parts of the glaciers (Fig. 11). The lower water vapor supply combined with the suppressing effect of cold glacier surfaces on convection contributes to a reduction in the precipitation over the glacierized areas. The modeling quantified this reduction as a notable 6.5 mm day^{-1} (37.2% of the simulation with glaciers present) at the glacier-dominated high elevations ($\geq$6000 m asl) (Fig. 12). Interestingly, the opposite of the aforementioned modeling results (more precipitation at higher elevations) occurs if glaciers are absent.

4.3. Evidence from isotopic analyses

The elevational dependence of *d*-excess in precipitation during the monsoon season (June–September) was investigated using the precipitation sampling network for stable isotopes in the Khumbu valley (Table. 2). Of special interest is the depletion in *d*-excess from Khunde (3874 m asl) to Lobuche (5050 m asl), which interrupts an otherwise increasing trend with elevation. The left tailed two-sample *t*-test for the *d*-excess values at Lobuche and Khunde indicates a significant depletion (p= 0.015). The local effects of below-cloud evaporation on stable isotope compositions of raindrops are considered to be a probable cause of this depletion, since *d*-excess decreases as ^{18}O becomes enriched when raindrops fall through unsaturated air (Gat and Tzur, 1967; Stewart, 1975). This can be further linked to the convergence near glacier fronts around 5000 m asl. The relative humidity of monsoonal flows is lowered

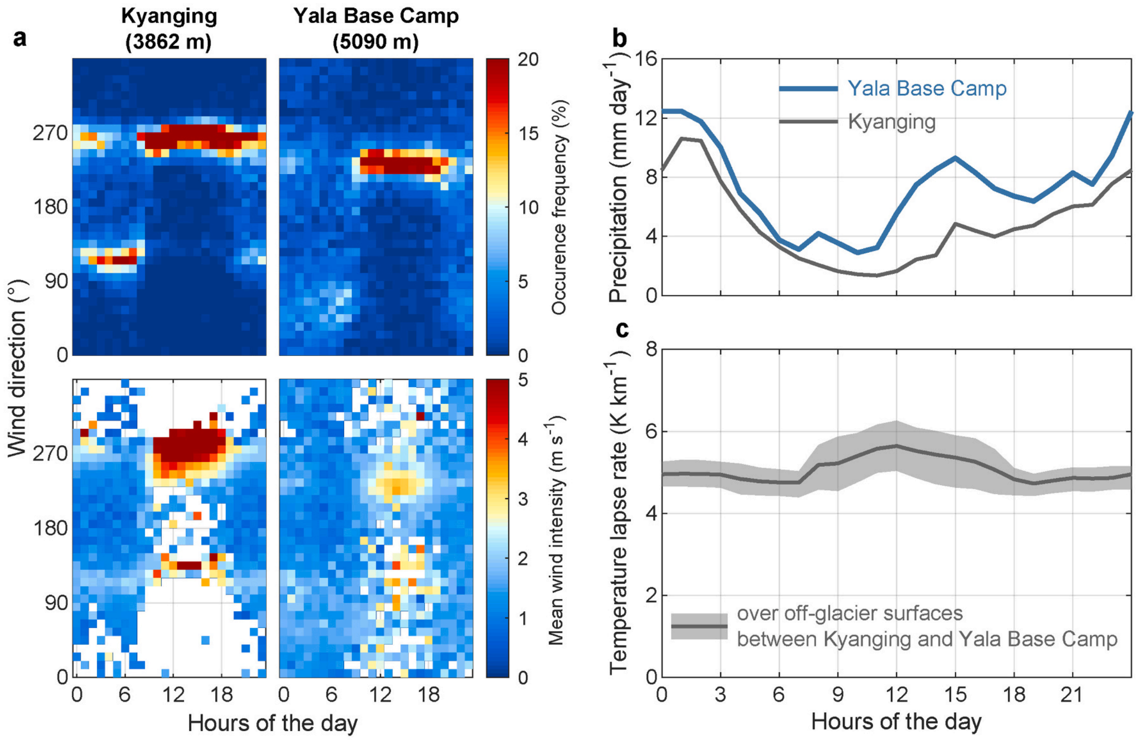

Fig. 6. Similar to Fig. 5 but for the observation network in the Langtang valley in summer (June–August) during 2012–2014.

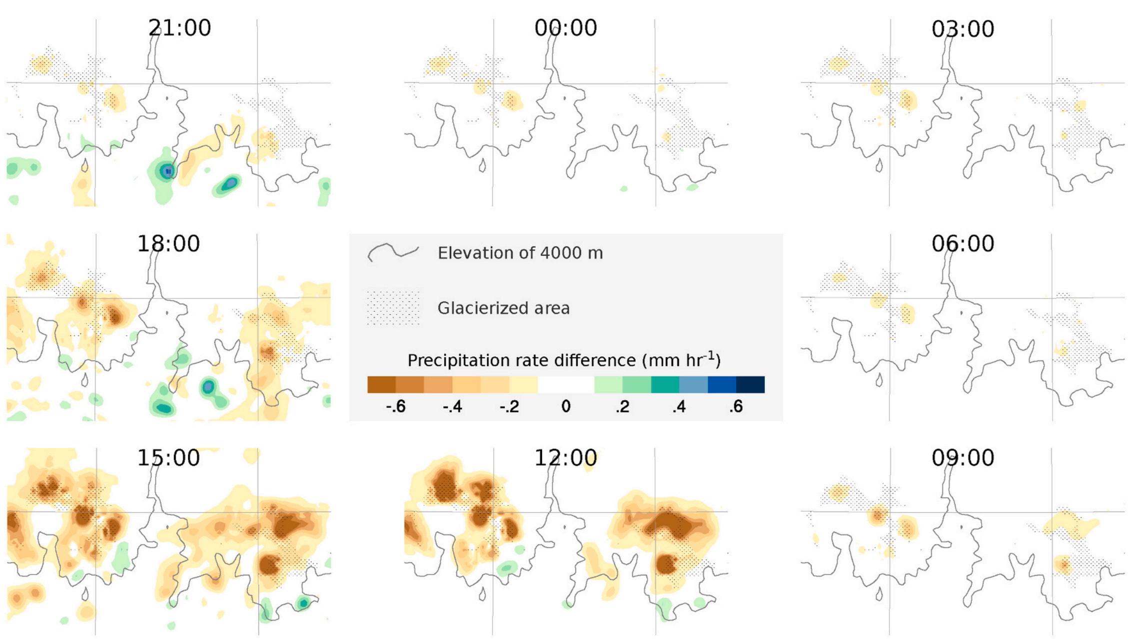

Fig. 7. Simulated diurnal cycle of the precipitation difference ('glacier case' minus 'non-glacier case'). The thin black contours denote the elevation of 4000 m. The dotted pattern represents the grid cells specified as land use type of 'SNOW/ICE'.

by the dry katabatic winds, thereby facilitating the partial evaporation of raindrops below the cloud base and in turn decreasing the *d*-excess in local precipitation.

This glacial influence on *d*-excess is further supported by our analysis of the isotope compositions in precipitation sampled at Pyramid (Table. 3). According to the two criteria ($C_i \geq 50\%$ and $C_{ii} \geq 50\%$) defined in Section 3.3, 16 precipitation samples were more likely attributed to glacial-effect events and another 17 were related to non-glacial-effect events ($C_i \geq 50\%$ and $C_{ii} \geq 50\%$). The remaining samples were considered to be mixed events (not clearly belonging to either group). On average, the glacial-effect and non-glacial-effect precipitation events had *d*-excess values of 10.97±2.91‰ and 12.48±2.34‰, respectively. The left tailed two-sample *t*-test for the difference between the two groups of *d*-excess values was significant at the 10% confidence level (p= 0.054), indicating that the *d*-excess of glacial-effect precipitation events is lower than that of non-glacial-effect events. Furthermore, compared with non-glacier-effect precipitation events, glacier-effect ones are associated with higher cloud base altitudes and lower relative

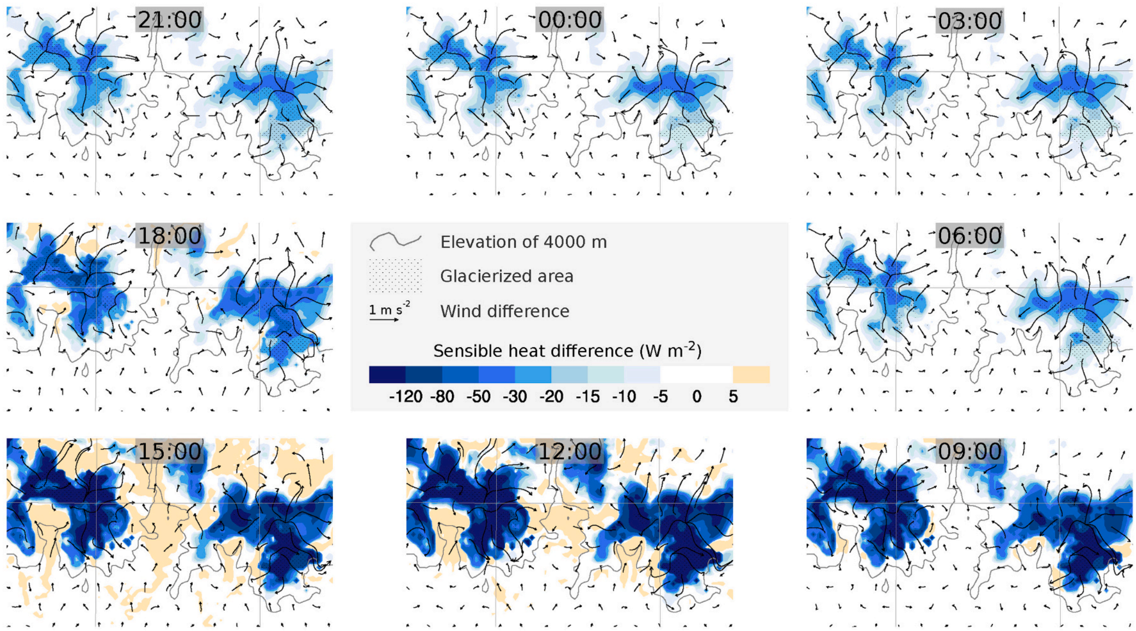

Fig. 8. Same as in Fig. 7 but for sensible heat flux (colors) and 10-m wind (arrows).

humidity (Table. 3), which favor re-evaporation of raindrops. The difference is significant between the two types of precipitation events for both parameters.

Overall, the isotopic analyses presented here are in line with our hypothesized mechanism in which precipitation near glacier fronts is promoted by the convergence between glacier winds and monsoonal flows.

5. Discussion

5.1. Uncertainties associated with the results

It is worth mentioning that observed phenomena represent the final consequence coming after a series of natural processes. Apart from the glacier effect, many other factors (e.g., local orography, contrast of land use/cover) may also contribute to the elevational dependence and diurnal cycle regarding some variables analyzed in this study. For example, the TLR is especially sensitive to the contrast of land use/cover. We noticed that the diurnal cycles of TLR between Namche and Pheriche and between Pheriche and Pyramid vary intensively (and opposite to each other), which differs notably from the TLRs of other combinations over off-glacier surfaces. This is due to the strong sensible heat flux associated with the land cover of alpine tundra at Pheriche. In spite of the aforementioned issue, the daytime sharp decrease is exclusively observed in the TLR over glacier surfaces, which is further seen in the results of the modeling experiment. Moreover, the integrated analysis of all of the information regarding precipitation, wind, and TLR presents compelling evidence supporting the hypothesized glacier effect on local precipitation.

Similarly, multiple processes control *d*-excess. Because *d*-excess records the difference between the actual δD and the expected equilibrium value based on measured δ^{18}O (Dansgaard, 1964), it is a measure of non-equilibrium isotopic effect and is therefore sensitive to kinetic fractionation processes, such as condensation at supersaturation and evaporation. It is not likely that the elevational dependence of mean *d*-excess during summer monsoon season derived from the five sites in the Khumbu valley (Table 2) is influenced by the oceanic water vapor source since the distance between the sites is limited. The in-cloud processes including the gradual rainout and recycling during water vapor transport (Froehlich et al., 2008; Guan et al., 2013; Peng et al., 2005) may explain the trend of increasing *d*-excess with elevation, whereas the depletion from Khunde to Lobuche is very likely the result of partial evaporation below cloud base (Gat and Tzur, 1967; Stewart, 1975). This is further supported by the association among *d*-excess, cloud base altitude, and relative humidity regarding glacier-effect and non-glacier-effect precipitation events. Thus, the subcloud processes are in line with the hypothesized convergence near glacier fronts, although more investigation may be necessary to further directly relate the two.

In contrast to observational data which record mixed impacts of a series of natural processes, models are a flexible tool for investigating a specific process of interest. In this study, the only difference between the control and sensitivity simulations is the presence of ‘glacier surface cooling’, allowing us to specifically investigate the effects of glacier-air interactions by comparing the two simulations. However, like any modeling studies, our approach also have caveats and limitations, especially when trying to quantify the extent to which this negative feedback may influence the lifetime of the Himalayan glaciers. First, the sensitivity simulation (‘non-glacier case’) was driven by current climate conditions, which may differ markedly from those of the future climate. However, of note is that the sensitivity case was not designed as a realistic simulation in which glaciers completely vanish in a warmer future. In fact, the experiment designed in this study represents a simplified but effective approach to ensure that the simulation differences are solely caused by glacier-air interactions. Second, a solid validation of the control simulation against observational data is not available, mainly due to the fact that the 2-km resolution still cannot realistically represent the complex relief of terrain and the heterogeneity of land use/cover types in this region, which to some extent shape the elevational dependence and diurnal cycle of variables investigated within the study. A very high resolution (as fine as 500 m) is probably needed to reproduce observed values (Bonekamp et al., 2018), while a 2-km resolution simulation can reproduce the general precipitation pattern (Lin et al., 2018). Thus, although a difference in precipitation was noted between the two modeling runs with and without the presence of glaciers (Fig. 12), it represents the strength of the negative feedback effect under the current climate conditions with undetermined uncertainties. In addition, this addresses the considerable uncertainties associated with the existing projections of future glacier changes obtained using models with coarser resolutions.

Similar modeling experiments have been conducted by Potter et al.

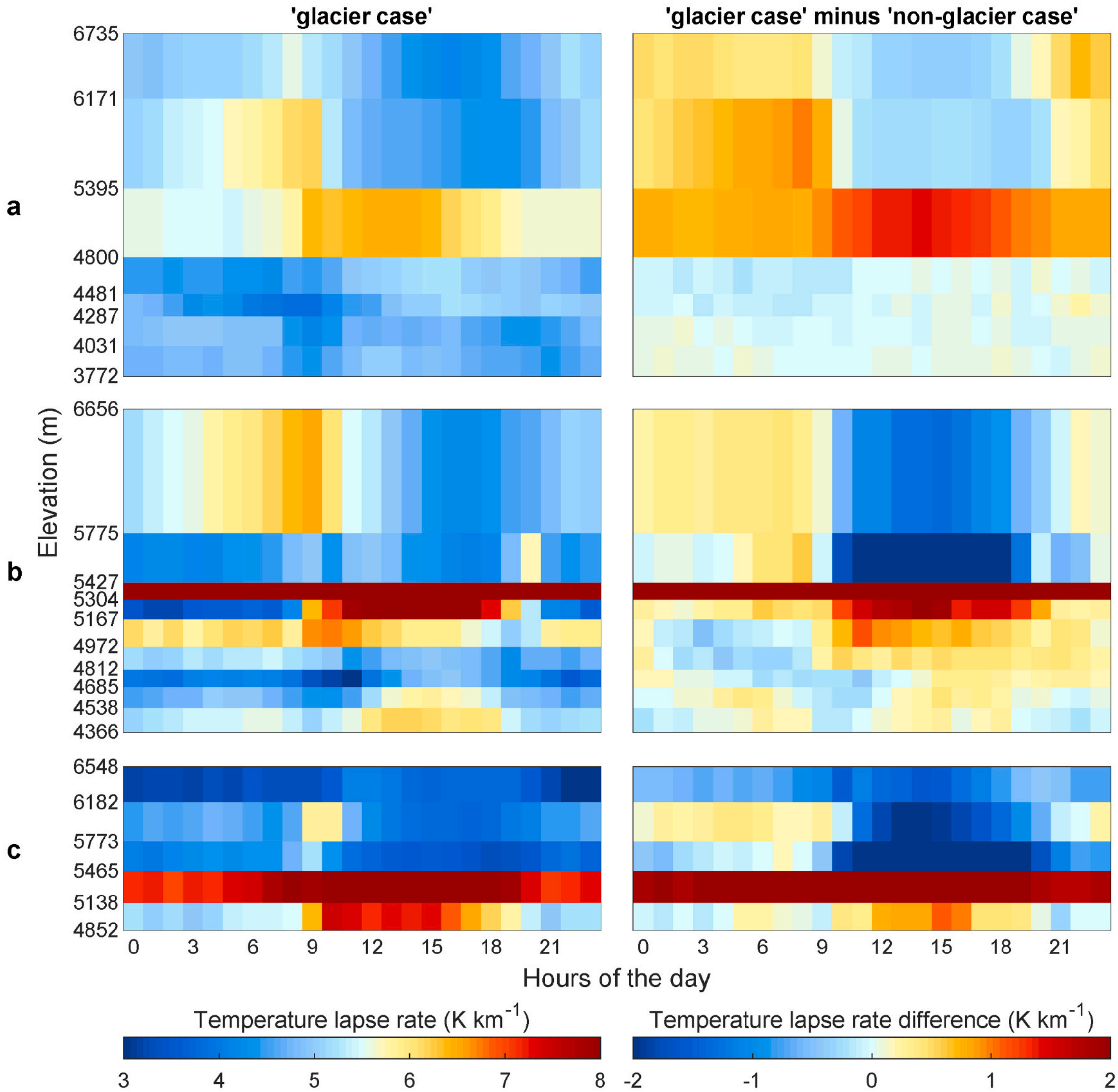

Fig. 9. Simulated diurnal cycle of the temperature lapse rate from 'glacier case' (left) and its difference to 'non-glacier case' (right) along the three south-north orientated sections correspondingly labeled 'a', 'b', and 'c' in Fig. 3.

(2018) and Ren et al. (2020) with different foci. Particularly focusing on the Khumbu valley using 1-km modeling experiments, Potter et al. (2018) concluded that the glacier cooling effect dampens the daytime up-valley winds based on the fact that the removal of glaciers from the model leads to the up-valley winds advancing further. Ren et al. (2020) reported that glacier absence would cause more than a 20% increase in precipitation in the high-elevation area in the southeastern TP. These independent modeling studies provide a sort of validation of our findings, pointing out that the lower modeling resolution (2-km) used in this study does not influence the interpretation of results related to the local wind circulation due to the cooing effect of glacier surfaces and concerning the change of precipitation pattern in case of glacier surface changes.

Despite the above shortcomings, our modeling results, along with the in situ meteorological and isotopic analyses, clearly demonstrate the proposed feedback.

5.2. Possible implications for the lifetime of the Himalayan glaciers

Our findings point out a negative feedback mechanism mediated by glacier-air interactions, i.e., the retreat (or complete loss, as in the sensitivity experiment) of glaciers attenuates the retarding effect of glacier winds on monsoonal flows, thereby enabling moist air to penetrate further up-valley and to enhance snow accumulation across the upper parts of glaciers. The negative feedback may, to some extent, mitigate the threat of future warming, hence extending the lifetime of Himalayan glaciers. In addition, the attenuated retardation of up-valley monsoonal flows by down-valley glacier winds may allow more of the water vapor transported by the Asian summer monsoon to reach the southern Tibetan Plateau (i.e., opposite values in Fig. 10), amplifying the observed wetting trend in the region (Lu et al., 2015).

The hypothesized mechanism postulated in this study is not subject to any special conditions other than daytime up-valley winds bringing plenty of water vapor for precipitation. Therefore, the mechanism should theoretically work in regions similar to the Khumbu region, for which the comprehensive observational evidence is provided in this study. Indeed, we obtained similar results from limited observations in the Langtang valley. Our simulations also indicate that the hypothesized mechanism works across the modeling domain since the glacier-effect precipitation commonly occurs in the areas below glacier fronts and thus is not limited to the Khumbu region (Fig. 7). Further evidence may come from the modeling study conducted on the southeastern Tibetan Plateau (Ren et al., 2020), which reveals that more precipitation would occur in the high-elevation area as a consequence of glacier loss, similar

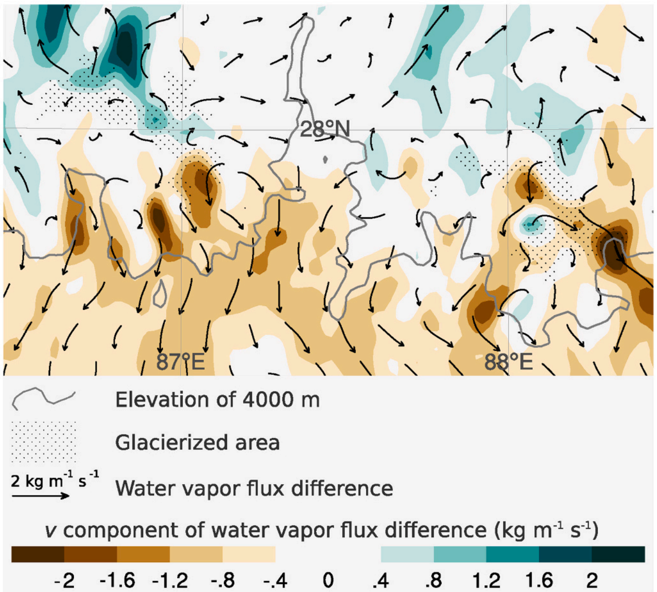

Fig. 10. Simulated difference ('glacier case' minus 'non-glacier case') in daily-mean water vapor flux (arrows) and its *v* component (colors).

to our modeling results.

Similarly, the hypothesized glacier effects should be effective in spite of the status of the Himalayan glaciers if the region is influenced by the Asian summer monsoon. Here we discuss the factors that may affect the magnitude of the feedback effect. We assessed the dynamic and thermodynamic conditions based on our modeling experiments. It was observed that the divergence (convergence) of the horizontal wind anomalies (Supplementary Fig. S3a), downward (upward) wind anomalies (Supplementary Fig. S3b), and negative (positive) precipitation anomalies (Fig. 7) generally exhibited similar but not perfectly (everywhere) matching patterns. The overall background of water vapor conditions (Supplementary Fig. S4) should be taken into account since abundant water vapor (provided by the monsoonal flows) is another critical factor affecting precipitation and explains why precipitation around the glacier fronts favored by the glacial effect is not predicted over the northern Himalayan slopes, where the air is dry (Wang et al., 2019). This indicates that the varying dominance of the Asian summer monsoon may also affect the magnitude of the feedback effect. However, the change in the monsoon system under climate warming is a complex issue that is beyond the scope of this study. The variation in the strength of katabatic winds with the retreat of glaciers could be another factor affecting the magnitude of the feedback effect. However, it is worth mentioning that katabatic winds will not necessarily be weakened as glaciers retreat under climate warming. Indeed, the temperature gradient between air and glacier surfaces may increase with climate warming further enhancing katabatic winds.

The mass budget of glaciers is determined by the difference between accumulation and ablation (i.e., roughly the combined effects of precipitation and temperature). The observed retreat of Himalayan glaciers is partly attributed to a precipitation reduction in summer (Salerno et al., 2015; Yao et al., 2012), indicating that precipitation changes deserve special attention along with warming when assessing the future fate of the Himalayan glaciers. Thus, the phase of precipitation could be an important factor because it affects the accumulation process. Indeed, we conducted an additional simulation with snow removed from the initial conditions but without forcing precipitation to be liquid (otherwise configured the same as the simulations presented in the study) and found that new snow is accumulated over high-elevation areas days after the simulation began. Therefore, assuming no dramatic warming, precipitation anomaly resulting from glacier retreat via the negative feedback is most likely solid due to the very high elevations.

Finally, a realistic representation of this feedback will require a coupled atmosphere-glacier mass balance model with sufficiently fine resolution, and no such model has yet been deployed in projections of future glacier changes, suggesting that the current projections may overestimate the rate of glacier retreat in the Himalayas.

6. Conclusions

We propose a mechanism that is mediated by summer glacier-air interactions. It enhances precipitation near glacier fronts due to the front-like convergence between cold, dry glacier winds and warm, moist monsoonal flows. By contrast, the mechanism suppresses precipitation at glacier-dominated high elevations, due to the reduced availability of

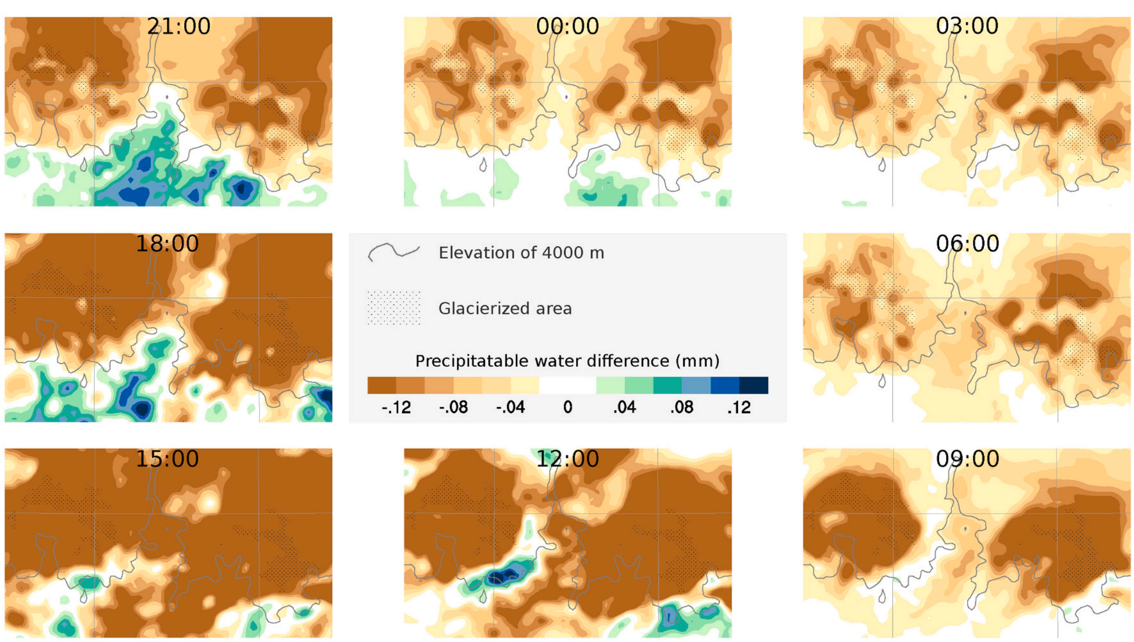

Fig. 11. Same as in Fig. 7 but for precipitable water.

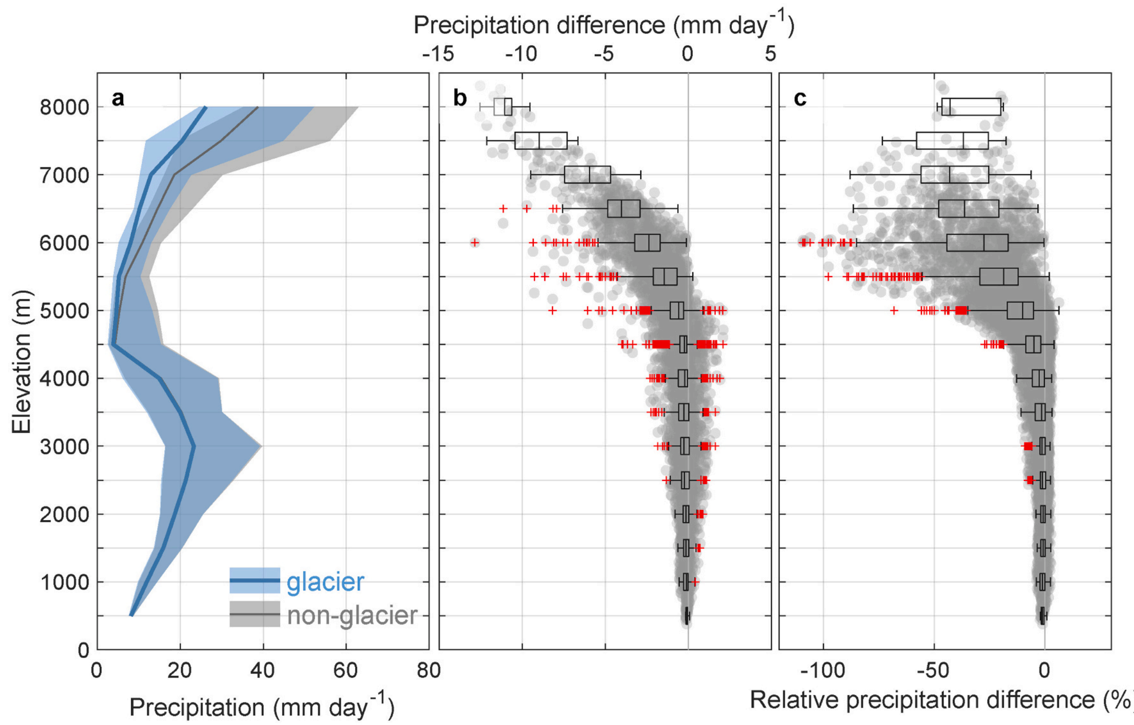

Fig. 12. Simulated effects of glacier loss on precipitation over the whole region of investigation. (**a**) Elevational dependence of precipitation simulated by the two modeling cases. The median (thick line), 25th- and 75th- percentiles (boundaries of colored area) are derived from grid cells in every 500-m wide elevational bins centered at 500 m intervals from 500 m asl. (**b**) Box-plot for precipitation difference ('glacier case' minus 'non-glacier case'; light-gray dots underneath) in the same bins as those of (**a**). Box boundaries represent 25th- and 75th- percentiles, and the line inside box is the median. Outliers marked with red plus signs lie beyond the whisker lengths (1.5 times the interquartile range away from the box boundaries). (**c**) Similar to (**b**) but for precipitation difference relative to that simulated by the 'glacier case'.

Table 2
Elevational dependence of $\delta^{18}O$, δD, and *d*-excess of the precipitation along the Khumbu valley in the summer monsoon season (June–September) during 2014–2017. Presented statistics regarding *d*-excess include mean and standard deviation (SD) for each site, and the *t*, *p* values of one tailed two-sample Student's *t*-test between every two neighboring sites. N is the sample size.

Site	Elevation (m)	N	$\delta^{18}O$ (‰)	δD (‰)	*d*-excess ()			
					Mean	SD	*t*	*p*
Lobuche	5050	62	−15.16	−112.07	9.21	6.07	**−2.19**	**0.015**
Khunde	3874	53	−12.67	−90.10	11.26	3.29	0.36	0.361
Lukla	2843	84	−8.98	−60.79	11.05	3.35	3.38	<0.001
Diktel	1623	205	−7.54	−50.86	9.46	3.74	7.29	<0.001
Sihara	102	122	−5.46	−37.36	6.32	3.81		

Table 3
Glacial effect on *d*-excess in precipitation, associated cloud base altitude (in terms of $T_L - T_S$) and near-surface relative humidity (*RH*) at Pyramid Station in the summer monsoon season (June–September) during 2012–2014. Presented statistics include the mean and standard deviation (SD) of each type of precipitation events, and the *t*, *p* values of one tailed two-sample Student's *t*-test between the two types of events. N is the sample size.

Daily events	N	Mean	SD	*t*	*p*
		d-excess (‰)			
Glacier-effect	16	10.97	2.91	−1.66	0.054
Non-glacier-effect	17	12.48	2.34		
		$T_L - T_S$ (K)			
Glacier-effect	16	0.74	0.51	2.74	0.005
Non-glacier-effect	17	0.32	0.24		
		RH (%)			
Glacier-effect	16	95.91	2.69	−2.75	0.005
Non-glacier-effect	17	98.20	1.38		

water vapor. The mechanism is well supported by three independent sources of evidence derived from in situ observations and high-resolution modeling experiments.

First, a unique elevational dependence of precipitation was observed in summer at sites along the Khumbu valley. Pyramid (with landscape formed by glacier front) experienced more summer precipitation, with a higher daytime contribution, compared with neighboring stations. This could be associated with the convergence between glacier winds and monsoonal flows, as further indicated by the decrease in up-valley winds with increasing elevation and by the sharp decrease in the diurnal cycle of TLR approximately from 10:00 to 16:00 (Nepal Local Time). Glacier retreat would result in the upward movement of water vapor and flow convergence. Similar phenomena were also observed from the limited data recorded in the Langtang valley.

Second, the stable water isotope compositions of precipitation agree with the hypothesized processes. Deuterium excess in precipitation increased with increasing elevation, until reaching glacier fronts. The depletion in *d*-excess in precipitation above the glacier fronts can be explained by the convergence between glacier winds and monsoonal flows, which leads to the relative humidity of monsoonal flows being lowered by the dry glacier winds, thereby facilitating partial evaporation of raindrops below the cloud base which in turn decreases *d*-excess in local precipitation. Indeed, glacier-effect precipitation events were also found to be associated with lower *d*-excess, higher cloud base altitude, and lower relative humidity. Therefore, dry and cold katabatic winds over glaciers play an important role in the formation of precipitation near glaciers, and future glacier retreat may result in more precipitation at higher elevations.

Third, the comparison between the high-resolution modeling simulations with and without the presence of glaciers fully supports our hypothesis. It is clearly demonstrated that the existence of glaciers favors precipitation near glacier fronts but suppresses precipitation at glacier-dominated high elevations. The suppression effect on precipitation predicted by the experiment can be as large as approximately 40%. Therefore, if the glaciers retreat, more precipitation would occur in the upper parts of glaciers.

The investigated and verified mechanism represents a negative feedback effect in which the retreat of the Himalayan glaciers may locally increase precipitation, thereby enhancing snow accumulation on the upper parts of glaciers. Therefore, this mechanism may mitigate the effect of future warming on the glacier mass balance, suggesting that existing projections based on models that ignore glacier-air interactions may overestimate the rate of glacier retreat in the Himalayas.

Declaration of Competing Interest

The authors declare that they have no known competing financial interests or personal relationships that could have appeared to influence the work reported in this paper.

Acknowledgments

The meteorological data from the PYRAMID Observatory Laboratory are available at http://geonetwork.evk2cnr.org. The isotopic data are available through Acharya (2018) and Balestrini et al. (2016).

This work was supported by the Strategic Priority Research Program of Chinese Academy of Sciences (Grant No. XDA2006010201 and No. XDA2006040103), the Second Tibetan Plateau Scientific Expedition and Research Program (Grant No. 2019QZKK0206), and the Swedish FORMAS, VR, VINOVVA, STINT, BECC, MERGE. The computations were performed on resources provided by the Swedish National Infrastructure for Computing (SNIC) at the National Supercomputer Centre in Sweden (NSC) partially funded by the Swedish Research Council through grant agreement no. 2018-05973. This work was also supported by the MIUR through the EV-K2-CNR/SHARE project within the framework of the EV-K2-CNR and Nepal Academy of Science and Technology (NAST). It is a contribution no 6 to CORDEX-FPS-CPTP.

We thank Kaji Bista, Giampietro Verza, and Agostino Da Polenza.

Appendix A. Supplementary data

Supplementary data to this article can be found online at https://doi.org/10.1016/j.atmosres.2021.105658.

References

Acharya, S., 2018. Altitude Dependence Study of Stable Isotopes in Precipitation along Southern Side of Himalayas. Doctor dissertation. University of Chinese Academy of Sciences, Beijing, China.

Aemisegger, F., Pfahl, S., Sodemann, H., Lehner, I., Seneviratne, S.I., Wernli, H., 2014. Deuterium excess as a proxy for continental moisture recycling and plant transpiration. Atmos. Chem. Phys. 14 https://doi.org/10.5194/acp-14-4029-2014.

Ageta, Y., Higuchi, K., 1984. Estimation of mass balance components of a summer-accumulation type glacier in the Nepal Himalaya. Geografiska Annaler: Series A, Physical Geography 66, 249–255. https://doi.org/10.1080/04353676.1984.11880113.

Balestrini, R., Delconte, C.A., Sacchi, E., Wilson, A.M., Williams, M.W., Cristofanelli, P., Putero, D., 2016. Wet deposition at the base of Mt Everest: Seasonal evolution of the chemistry and isotopic composition. Atmos. Environ. 146, 100–112. https://doi.org/10.1016/j.atmosenv.2016.08.056.

Barnett, T.P., Adam, J.C., Lettenmaier, D.P., 2005. Potential impacts of a warming climate on water availability in snow-dominated regions. Nature 438, 303–309. https://doi.org/10.1038/nature04141.

Bolch, T., Kulkarni, A., Kääb, A., Huggel, C., Paul, F., Cogley, J., Frey, H., Kargel, J.S., Fujita, K., Scheel, M., et al., 2012. The state and fate of Himalayan glaciers. Science 336, 310–314. https://doi.org/10.1126/science.1215828.

Bolton, D., 1980. The computation of equivalent potential temperature. Mon. Weather Rev. 108, 1046–1053. https://doi.org/10.1175/1520-0493(1980)108<1046:TCOEPT>2.0.CO;2.

Bonekamp, P., Collier, E., Immerzeel, W., 2018. The impact of spatial resolution, land use, and spinup time on resolving spatial precipitation patterns in the Himalayas. J. Hydrometeorol. 19, 1565–1581. https://doi.org/10.1175/JHM-D-17-0212.1.

Bookhagen, B., Burbank, D.W., 2010. Toward a complete Himalayan hydrological budget: Spatiotemporal distribution of snowmelt and rainfall and their impact on river discharge. J. Geophys. Res. Earth Surf. 115 https://doi.org/10.1029/2009JF001426.

Collier, E., Maussion, F., Nicholson, L.I., Mölg, T., Immerzeel, W.W., Bush, A.B.G., 2015. Impact of debris cover on glacier ablation and atmosphere–glacier feedbacks in the Karakoram. Cryosphere 9, 1617–1632. https://doi.org/10.5194/tc-9-1617-2015.

Conway, J., Helgason, W., Pomeroy, J., Sicart, J., 2021. Icefield breezes: mesoscale diurnal circulation in the atmospheric boundary layer over an outlet of the Columbia Icefield, Canadian Rockies. J. Geophys. Res.-Atmos. https://doi.org/10.1029/2020JD034225 e2020JD034225.

Dansgaard, W., 1964. Stable isotopes in precipitation. Tellus 16, 436–468. https://doi.org/10.3402/tellusa.v16i4.8993.

Dee, D., Uppala, S., Simmons, A., Berrisford, P., Poli, P., Kobayashi, S., Andrae, U., Balmaseda, M., Balsamo, G., Bauer, P., et al., 2011. The ERA-Interim reanalysis: Configuration and performance of the data assimilation system. Q. J. R. Meteorol. Soc. 137, 553–597. https://doi.org/10.1002/qj.828.

Froehlich, K., Kralik, M., Papesch, W., Rank, D., Scheifinger, H., Stichler, W., 2008. Deuterium excess in precipitation of Alpine regions–moisture recycling. Isot. Environ. Health Stud. 44, 61–70. https://doi.org/10.1080/10256010801887208.

Gardner, A.S., Moholdt, G., Cogley, J.G., Wouters, B., Arendt, A.A., Wahr, J., Berthier, E., Hock, R., Pfeffer, W.T., Kaser, G., et al., 2013. A reconciled estimate of glacier contributions to sea level rise: 2003 to 2009. Science 340, 852–857. https://doi.org/10.1126/science.1234532.

Gat, J., Tzur, Y., 1967. Modification of the isotopic composition of rainwater by processes which occur before groundwater recharge. In: Isotopes in Hydrology. Proceedings of a Symposium, International Atomic Energy Agency (IAEA), Vienna, Austria, pp. 49–60.

Guan, H., Zhang, X., Skrzypek, G., Sun, Z., Xu, X., 2013. Deuterium excess variations of rainfall events in a coastal area of South Australia and its relationship with synoptic weather systems and atmospheric moisture sources. J. Geophys. Res.-Atmos. 118, 1123–1138. https://doi.org/10.1002/jgrd.50137.

Hock, R., Bliss, A., Marzeion, B., Giesen, R.H., Hirabayashi, Y., Huss, M., Radić, V., Slangen, A.B.A., 2019. GlacierMIP–a model intercomparison of global-scale glacier mass-balance models and projections. J. Glaciol. 65, 453–467. https://doi.org/10.1017/jog.2019.22.

Hren, M.T., Bookhagen, B., Blisniuk, P.M., Booth, A.L., Chamberlain, C.P., 2009. δ^{18}O and δD of streamwaters across the Himalaya and Tibetan Plateau: Implications for moisture sources and paleoelevation reconstructions. Earth Planet. Sci. Lett. 288, 20–32. https://doi.org/10.1016/j.epsl.2009.08.041.

Immerzeel, W.W., Van Beek, L.P., Bierkens, M.F., 2010. Climate change will affect the Asian water towers. Science 328, 1382–1385. https://doi.org/10.1126/science.1183188.

Immerzeel, W.W., Lutz, A., Andrade, M., Bahl, A., Biemans, H., Bolch, T., Hyde, S., Brumby, S., Davies, B., Elmore, A., et al., 2020. Importance and vulnerability of the world's water towers. Nature 577, 364–369. https://doi.org/10.1038/s41586-019-1822-y.

Karki, R., Hasson, S., Gerlitz, L., Schickhoff, U., Scholten, T., Böhner, J., 2017. Quantifying the added value of convection-permitting climate simulations in complex terrain: a systematic evaluation of WRF over the Himalayas. Earth System Dynam. 8, 507–528. https://doi.org/10.5194/esd-8-507-2017.

Kaser, G., Großhauser, M., Marzeion, B., 2010. Contribution potential of glaciers to water availability in different climate regimes. Proc. Natl. Acad. Sci. 107, 20223–20227. https://doi.org/10.1073/pnas.1008162107.

Kraaijenbrink, P., Bierkens, M., Lutz, A., Immerzeel, W., 2017. Impact of a global temperature rise of 1.5 degrees Celsius on Asia's glaciers. Nature 549, 257–260. https://doi.org/10.1038/nature23878.

Lin, C., Chen, D., Yang, K., Ou, T., 2018. Impact of model resolution on simulating the water vapor transport through the central himalayas: implication for models' wet bias over the Tibetan Plateau. Clim. Dyn. 51, 3195–3207. https://doi.org/10.1007/s00382-018-4074-x.

Lu, N., Trenberth, K.E., Qin, J., Yang, K., Yao, L., 2015. Detecting long-term trends in precipitable water over the tibetan plateau by synthesis of station and MODIS observations. J. Clim. 28, 1707–1722. https://doi.org/10.1175/JCLI-D-14-00303.1.

Lutz, A., Immerzeel, W., Shrestha, A., Bierkens, M., 2014. Consistent increase in High Asia's runoff due to increasing glacier melt and precipitation. Nat. Clim. Chang. 4, 587–592. https://doi.org/10.1038/nclimate2237.

Masson-Delmotte, V., Jouzel, J., Landais, A., Stievenard, M., Johnsen, S.J., White, J., Werner, M., Sveinbjornsdottir, A., Fuhrer, K., 2005. GRIP deuterium excess reveals rapid and orbital-scale changes in Greenland moisture origin. Science 309, 118–121. https://doi.org/10.1126/science.1108575.

Maurer, J.M., Schaefer, J., Rupper, S., Corley, A., 2019. Acceleration of ice loss across the Himalayas over the past 40 years. Sci. Adv. 5 https://doi.org/10.1126/sciadv.aav7266 eaav7266.

Mölg, T., Großhauser, M., Hemp, A., Hofer, M., Marzeion, B., 2012. Limited forcing of glacier loss through land-cover change on Kilimanjaro. Nat. Clim. Chang. 2, 254–258. https://doi.org/10.1017/jog.2019.22.

Norris, J., Carvalho, L.M., Jones, C., Cannon, F., Bookhagen, B., Palazzi, E., Tahir, A.A., 2017. The spatiotemporal variability of precipitation over the himalaya: evaluation of one-year WRF model simulation. Clim. Dyn. 49, 2179–2204. https://doi.org/10.1007/s00382-016-3414-y.

Peng, H., Mayer, B., Norman, A.L., Krouse, H.R., 2005. Modelling of hydrogen and oxygen isotope compositions for local precipitation. Tellus Ser. B Chem. Phys. Meteorol. 57, 273–282. https://doi.org/10.3402/tellusb.v57i4.16545.

Potter, E.R., Orr, A., Willis, I.C., Bannister, D., Salerno, F., 2018. Dynamical drivers of the local wind regime in a Himalayan valley. J. Geophys. Res.-Atmos. 123, 13–186. https://doi.org/10.1029/2018JD029427.

Radić, V., Hock, R., 2011. Regionally differentiated contribution of mountain glaciers and ice caps to future sea-level rise. Nat. Geosci. 4, 91–94. https://doi.org/10.1038/ngeo1052.

Ren, W., Yao, T., Xie, S., 2017. Key drivers controlling the stable isotopes in precipitation on the leeward side of the Central Himalayas. Atmos. Res. 189, 134–140. https://doi.org/10.1016/j.atmosres.2017.01.020.

Ren, L., Duan, K., Xin, R., 2020. Impact of future loss of glaciers on precipitation pattern: a case study from south-eastern Tibetan Plateau . Atmos. Res. 242, 104984. Doi: https://doi.org/10.1016/j.atmosres.2020.104984.

Salerno, F., Guyennon, N., Thakuri, S., Viviano, G., Romano, E., Vuillermoz, E., Cristofanelli, P., Stocchi, P., Agrillo, G., Ma, Y., et al., 2015. Weak precipitation, warm winters and springs impact glaciers of south slopes of Mt. Everest (central Himalaya) in the last 2 decades (1994–2013). Cryosphere 9, 1229–1247. https://doi.org/10.5194/tc-9-1229-2015.

Salerno, F., Thakuri, S., Tartari, G., Nuimura, T., Sunako, S., Sakai, A., Fujita, K., 2017. Debris-covered glacier anomaly? Morphological factors controlling changes in the mass balance, surface area, terminus position, and snow line altitude of Himalayan glaciers. Earth Planet. Sci. Lett. 471, 19–31. https://doi.org/10.1016/j.epsl.2017.04.039.

Shannon, S., Smith, R., Wiltshire, A., Payne, T., Huss, M., Betts, R., Caesar, J., Koutroulis, A., Jones, D., Harrison, S., 2019. Global glacier volume projections under high-end climate change scenarios. Cryosphere 13, 325–350. https://doi.org/10.5194/tc-13-325-2019.

Shaw, T.E., Yang, W., Ayala, Á., Bravo, C., Zhao, C., Pellicciotti, F., 2021. Distributed summer air temperatures across mountain glaciers in the south-east Tibetan Plateau: temperature sensitivity and comparison with existing glacier datasets. Cryosphere 15, 595–614. https://doi.org/10.5194/tc-15-595-2021.

Shea, J.M., Wagnon, P., Immerzeel, W.W., Biron, R., Brun, F., Pellicciotti, F., 2015. A comparative high-altitude meteorological analysis from three catchments in the Nepalese Himalaya. Int. J. Water Res. Develop. 31, 174–200. https://doi.org/10.1080/07900627.2015.1020417.

Skamarock, W.C., Klemp, J.B., Dudhia, J., Gill, D.O., Barker, D.M., Duda, M.G., Huang, X. Y., Wang, W., Powers, J.G., 2008. A description of the Advanced Research WRF version 3. Technical Report. NCAR/TN-475+STR. https://doi.org/10.5065/D68S4MVH.

Stewart, M.K., 1975. Stable isotope fractionation due to evaporation and isotopic exchange of falling waterdrops: applications to atmospheric processes and evaporation of lakes. J. Geophys. Res. 80, 1133–1146. https://doi.org/10.1029/JC080i009p01133.

Tian, L., Masson-Delmotte, V., Stievenard, M., Yao, T., Jouzel, J., 2001. Tibetan Plateau summer monsoon northward extent revealed by measurements of water stable isotopes. J. Geophys. Res.-Atmos. 106, 28081–28088. https://doi.org/10.1029/2001JD900186.

Tian, L., Yao, T., White, J., Yu, W., Wang, N., 2005. Westerly moisture transport to the middle of himalayas revealed from the high deuterium excess. Chin. Sci. Bull. 50, 1026–1030. https://doi.org/10.1007/s11434-005-1026-8.

Wang, Y., Yang, K., Zhou, X., Wang, B., Chen, D., Lu, H., Lin, C., Zhang, F., 2019. The formation of a dry-belt in the north side of central Himalaya Mountains. Geophys. Res. Lett. 46, 2993–3000. https://doi.org/10.1029/2018GL081061.

Yang, K., Guyennon, N., Ouyang, L., Tian, L., Tartari, G., Salerno, F., 2018. Impact of summer monsoon on the elevation-dependence of meteorological variables in the south of central Himalaya. Int. J. Climatol. 38, 1748–1759. https://doi.org/10.1002/joc.5293.

Yao, T., Thompson, L., Yang, W., Yu, W., Gao, Y., Guo, X., Yang, X., Duan, K., Zhao, H., Xu, B., et al., 2012. Different glacier status with atmospheric circulations in Tibetan Plateau and surroundings. Nat. Clim. Chang. 2, 663–667. https://doi.org/10.1038/nclimate1580.

Yu, W., Yao, T., Tian, L., Ma, Y., Wen, R., Devkota, L.P., Wang, W., Qu, D., Chhetri, T.B., 2016. Short-term variability in the dates of the Indian monsoon onset and retreat on the southern and northern slopes of the Central Himalayas as determined by precipitation stable isotopes. Clim. Dyn. 47, 159–172. https://doi.org/10.1007/s00382-015-2829-1.